

# On the Vulnerability of Deep Automatic Modulation Classifiers to Explainable Backdoor Threats

Younes Salmi  
Institute of Radiocommunications  
Poznan University of Technology  
Poznań, Poland  
younes.salmi@put.poznan.pl

Hanna Bogucka  
Institute of Radiocommunications  
Poznan University of Technology  
Poznań, Poland  
hanna.bogucka@put.poznan.pl

**Abstract**—Deep learning (DL) has been widely studied for assisting applications of modern wireless communications. One of the applications is automatic modulation classification (AMC). However, DL models are found to be vulnerable to adversarial machine learning (AML) threats. One of the most persistent and stealthy threats is the backdoor (Trojan) attack. Nevertheless, most studied threats originate from other AI domains, such as computer vision (CV). Therefore, in this paper, a physical backdoor attack targeting the wireless signal before transmission is studied. The adversary is considered to be using explainable AI (XAI) to guide the placement of the trigger in the most vulnerable parts of the signal. Then, a class prototype combined with principal components is used to generate the trigger. The studied threat was found to be efficient in breaching multiple DL-based AMC models. The attack achieves high success rates for a wide range of SNR values and a small poisoning ratio.

**Index Terms**—Backdoor attacks, modulation classification, explainable artificial intelligence.

## I. INTRODUCTION

Automatic Modulation Classification (AMC) is the process of identifying the modulation schemes of unknown wireless signals. Deep Learning (DL) models have demonstrated significant performance as feature-based AMC techniques. For instance, unsupervised learning algorithms such as auto-encoders (AE) are used to learn the hidden patterns in the IQ waveforms and determine the modulation scheme without relying on the ground-truth label. In supervised learning, Deep Neural Networks (DNN) are used to extract high-level features from the data, but they are limited in terms of capturing local dependencies [1]. In contrast, Convolutional Neural Networks (CNN) excel in detecting local patterns within the wireless data using two-dimensional filters [2]. Recurrent neural Networks (RNNs) are used to get the sequential dependencies in the IQ data samples modeled as time series [3].

Despite the eminence of the DL techniques, they are susceptible to a class of threats called adversarial machine learning (AML) threats [4]. Adversaries exploit vulnerabilities in the DL models, data, or training platforms to design stealthy and

efficient attacks. For example, threats such as membership inference attacks (MIA) are used to breach the privacy of the DL systems [5]. In MIA, the adversary aims to discover if a data sample is a part of the training dataset by analyzing the model’s outputs. Typically, exploiting differences in prediction confidence or loss values between seen (member) and unseen (non-member) samples. In addition, methods such as the fast gradient sign method (FGSM) [6] and Carlini-Wagner (C&W) [7] attacks are used in threats such as causative (poisoning) and evasion (adversarial examples) attacks to craft perturbations.

A new kind of AML attack, known as backdoor or Trojan attacks [8], has become widely discussed to address the vulnerabilities of DL-based AMC systems. In a backdoor attack, the adversary embeds perturbations in the training dataset (causative) to design the backdoor. This backdoor remains inactivated on legitimate samples during inference. To activate the backdoor, triggers are used by embedding the same perturbation used in the training in inference samples (evasion). This type of attack is considered more stealthy compared to causative and evasion attacks, because the attacked DL model maintains classification accuracy if the test (inference) data are clean (without a trigger).

In this paper, we study the first transferable position-aware backdoor attack on DL-based AMC. Explainable AI (XAI) is used to decide on the positions to embed the perturbations. To the best of our knowledge, XAI techniques have been only used to guide backdoor design in radio frequency (RF) fingerprinting [9]. Additionally, the literature lacks the transferability study of these threats in DL-based AMC. We focus on physical attacks that are designed on the baseband modulated signal before transmission, in contrast to the existing works that rely on digital data manipulation. The rest of this paper is organized as: Section II details the XAI-guided backdoor attack. Section III discusses the simulation results. The last section IV concludes the work.

## II. THE ATTACK MODEL

We consider the AMC system discussed in [10], with the same notations. Three models are chosen to classify the received signals into their modulations: a DNN [1], an RNN [2], and a CNN [11]. The backdoor attack consists of two phases. The first deals with position selection to embed the

perturbations, and a customized SamplingSHAP approach is employed for this purpose. Once these positions are selected, the second phase uses a Principal Component Analysis (PCA) technique named Prototype-PCA Hybrid to decide on the perturbation values. We study a black-box scenario where the adversary only has access to the training dataset  $\mathcal{D}_{\text{train}}$ . The model parameters  $\theta$ , model gradients, and internal architecture of the model  $f_\theta$  are considered unknown to the adversary.

### A. Trigger Position Selection

To determine the trigger positions, a customized SamplingSHAP is applied to compute feature attributions, but over grouped IQ time-domain samples of the input of the DL-based AMC system. These positions must be determined in the physical attack domain, i.e., before transmission of the time-domain OFDM signals. The adversary aims to identify a time window  $W^*$  where the model is most sensitive to data manipulations, in this case, perturbations. It is assumed that the adversary is unaware of the cyclic prefix (CP) length  $N_{cp}$ . Let  $N$  be the number of useful subcarriers, and  $\mathbf{S} = \{s_1, s_2, \dots, s_M\}$  be the set of  $M$  CP-inserted OFDM signals, where each  $s_m \in \mathbb{C}^{N+N_{cp}}$ . Given the real  $\Re(\mathbf{S})$  and imaginary  $\Im(\mathbf{S})$  components, the customized SamplingSHAP approach proceeds as follows.

To reduce the computations of SHAP, the complex IQ samples are grouped into non-overlapping windows of length  $N_w$  samples. For a single OFDM data symbol  $s \in \mathbb{C}^{N+N_{cp}}$ , the set of windows is:

$$\mathbf{W} = \{W_l \mid W_l = s[l \cdot N_w : (l+1) \cdot N_w - 1], \\ l = 0, \dots, L-1\}, \quad (1)$$

where  $L = \frac{N+N_{cp}}{N_w}$  is the number of windows per symbol.

The adversary aims to breach the system before the transmission of training signals; thus, the radio channel effects are not considered in designing the attack. However, these signals may exhibit arbitrary phase offsets from modulation mapping, pilot structure, or preprocessing steps. These offsets can bias the feature attribution process to absolute phase windows instead of discriminative intra-window structures. To avoid this, the adversary applies a local phase normalization to each window. For the  $l$ -th window  $W_l = \{W_l[0], W_l[1], \dots, W_l[N_w - 1]\}$ , the mean complex phasor is computed as follows:

$$\bar{p}_l = \frac{1}{N_w} \sum_{n=0}^{N_w-1} W_l[n], \quad (2)$$

and its dominant phase component is extracted as:

$$\phi_l = \angle(\bar{p}_l) = \arctan 2(\Im(\bar{p}_l), \Re(\bar{p}_l)). \quad (3)$$

The phase-normalized samples are then defined as:

$$\hat{W}_l[n] = W_l[n] \cdot e^{-j\phi_l}, \quad n = 0, \dots, N_w - 1. \quad (4)$$

This transformation rotates the entire window in the complex plane. Thus, the window's average phasor lies on the positive real axis; then, the reference phase is standardized across all training signals. As a result, the customized SamplingSHAP

relies on amplitude patterns and relative phase changes within the window, which are more informative and important for determining the positions of the triggers. Nevertheless, the trigger is designed in the normalized space; as a result, the original phase must be considered, and the original physical-domain samples are obtained as  $W_l[n] = \hat{W}_l[n] \cdot e^{j\phi_l}$ .

To ensure that the signal power will not differ significantly after manipulation, a background set  $\mathcal{B}$  is constructed of phase-normalized windows  $\hat{W}_l$  by sampling windows from both the target class  $y_{\text{tar}}$  and all non-target classes. The background is used to replace masked windows during SHAP sampling, preserving the validity of the time-domain signal.

Let  $z \in \{0, 1\}^L$  be a binary mask over the  $L$  phase-normalized windows, where  $z_l = 0$  indicates that the  $l$ -th window  $\hat{W}_l$  is replaced by a background window from  $\mathcal{B}$ , and  $z_l = 1$  indicates that the original window  $\hat{W}_l$  is retained. The perturbed symbol under the mask  $z$  is given by:

$$\tilde{s}^{(z)} = \text{merge}(\hat{W}_l, z_l, \mathcal{B}), \quad (5)$$

where  $\text{merge}(\cdot)$  performs element-wise replacement based on  $z$  and reconstructs the symbol. For  $y_{\text{tar}}$ , the SHAP value for window  $k$  is estimated using the following:

$$\phi_l = \frac{1}{\Upsilon} \sum_{s=1}^{\Upsilon} \left[ f_\theta \left( \tilde{s}^{(z_{+l}^{(v)})} \right) - f_\theta \left( \tilde{s}^{(z_{-l}^{(v)})} \right) \right]_{y_{\text{tar}}}, \quad (6)$$

where  $z_{+l}^{(v)}$  and  $z_{-l}^{(v)}$  differ in the inclusion of window  $l$  in the permutation  $v$ , and  $\Upsilon$  is the number of Monte Carlo samples.

The optimal trigger location is then selected as the window with the highest average SHAP value over all signals:

$$W_l^* = \arg \max_{W_l \in \mathbf{W}} \mathbb{E}_{s \sim \mathbf{S}}[\phi_l], \quad (7)$$

with the option of selecting the top-2 highest windows to improve robustness against varying the wireless channel.

### B. Trigger Value Generation

Once the trigger position  $W^*$  is determined, a combination of class prototypes and principal components is used to generate the value of the trigger. Let  $\mathbf{W}_{\text{tar}}$  be the set of all phase-normalized windows from  $W^*$  belonging to  $y_{\text{tar}}$ :

$$\mathbf{W}_{\text{tar}} = \{\hat{W} \mid (s, y) \in \mathcal{D}_{\text{train}}, y = y_{\text{tar}}, W^* \subset s\}. \quad (8)$$

The complex prototype vector  $\mu_{\text{tar}}$  is computed as median ( $\mathbf{W}_{\text{tar}}$ ) where the median is taken element-wise over the complex plane to increase robustness to outliers. A real-valued data matrix is formed:

$$\mathbf{S}_{\text{tar}} = \left[ \Re(\hat{W}), \Im(\hat{W}) \right], \quad \hat{W} \in \mathbf{W}_{\text{tar}}, \quad (9)$$

and compute the first principal component  $u_1$  from the covariance matrix:  $u_1 = \arg \max_{\|u\|_2=1} \text{Var}(\mathbf{S}_{\text{tar}} u)$ . The complex PCA direction  $p_{\text{tar}}$  is reconstructed from the real and imaginary halves of  $u_1$ . The final trigger vector is:

$$t = \alpha \cdot \frac{\lambda \mu_{\text{tar}} + (1 - \lambda) p_{\text{tar}}}{\|\lambda \mu_{\text{tar}} + (1 - \lambda) p_{\text{tar}}\|_2}, \quad (10)$$

where  $\lambda \in [0, 1]$  controls the mix between prototype and PCA, and  $\alpha$  controls the trigger energy.

### C. Causative Phase (Backdoor Insertion)

The backdoor attack starts with poisoning some of the training data before symbols. For a single training example, let  $J \subset \{0, 1, \dots, M-1\}$  be the indices of the poisoned symbols. Therefore, the symbol poisoning ratio is  $\rho_h = \frac{|J|}{M} \times 100\%$ . For each symbol  $m \in J$ , the samples in  $W^*$  are replaced as:

$$s_m^*[n] = \begin{cases} s_m[n] + t[n], & n \in W^*, \\ s_m[n], & \text{otherwise.} \end{cases} \quad (11)$$

The manipulated samples are then relabeled to  $y_{\text{tar}}$ . The poisoned set of OFDM symbols is denoted as  $\mathbf{S}^*$ , and its received version following the same transmission and reception processes as in the legitimate scenario is denoted as  $\mathbf{X}^*$ . The poisoned dataset  $\mathcal{D}_{\text{train}}^*$  is defined as:

$$\mathcal{D}_{\text{train}}^* = \{(s_m^*, y_{\text{tar}}) \mid m \in J\} \cup \{(s_m, y_m) \mid m \notin J\}. \quad (12)$$

Training the model on  $\mathcal{D}_{\text{train}}^*$  yields the backdoored model  $f_{\theta^*}$  parametrized by the backdoored parameters  $\theta^* \in \Theta^*$ . This backdoored model learn the following mapping:

$$f_{\theta^*} : \mathbb{R}^{M \times N \times 2} \rightarrow [0, 1]^{M \times N \times O}, \quad f_{\theta}(\mathbf{X}^*) = \mathbf{Y}. \quad (13)$$

### III. RESULTS AND DISCUSSIONS

For the simulation setup, the number of OFDM subcarriers is chosen to be  $N = 512$  with a CP of length  $N_{cp} = 128$ . The random phase  $\kappa_m$  was  $\mathcal{U}(0, 2\pi)$  per symbol. The Rapp smoothness was set to be 2, the IBO value 3dB, and three CNC iterations were employed to combat the PA distortions. A 3-tap Rayleigh fading channel with the delay path  $\{0, 2, 4\}$  was simulated. Eleven modulation types were used as discussed in [11]. A TTI of length  $M = 14$  OFDM symbols is selected. 100,000 examples were collected, and 80%-20% is the proportion for training-test examples.

For windowing, each  $s \in \mathbb{C}^{N+N_{cp}}$  is partitioned into non-overlapping windows of length  $N_w \in \{32, 64\}$ . With  $N + N_{cp} = 640$ , this yields  $L \in \{20, 10\}$  windows. The pool phase-normalized windows drawn 50% from the target class  $y_{\text{tar}}$  and 50% from non-targets. For each candidate window  $l$ , draw  $\Upsilon = 100$  Monte Carlo masks  $z \in \{0, 1\}^L$  and compute the marginal contribution to  $f_{\theta}(\cdot)_{y_{\text{tar}}}$  when toggling  $l$  (mask-and-replace with  $\mathcal{B}$ ). Per-class SHAP is averaged over 200 symbols per class. Sweeping  $\lambda \in \{0, 0.25, 0.5, 0.75, 1\}$  and  $\alpha$  chosen to meet a local energy budget:  $\alpha = \kappa \cdot \sqrt{\frac{1}{N_w} \sum_{n \in W^*} |s[n]|^2}$  with  $\kappa \in \{-24, -21, -18, -15\}$  dB relative to the window RMS.

To evaluate the adversarial threat, the ASR, the clean accuracy (ALC), and the benign accuracy (ABC) are defined as follows: Since the evaluation metrics are used to assess the DL models, the signals used in these metrics are the received version of the physical signals. ASR measures the proportion of triggered test signals  $x^* \in X_{\text{test}}^*$  that the backdoored model  $f_{\theta^*}$  misclassifies into the target class  $y_{\text{tar}}$ . ALC measures the classification accuracy of the legitimate (clean) model  $f_{\theta}$  on the clean test set  $\mathbf{X}_{\text{test}}$ . It serves as the baseline performance in the absence of any attack. ABC measures the classification

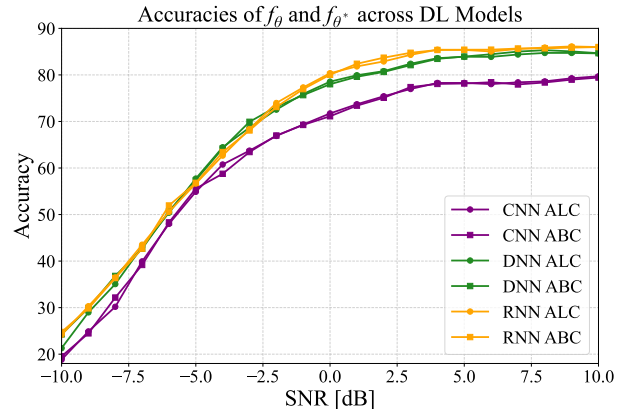


Fig. 1. ALC and ABC across the reference DNN, RNN, and CNN.

accuracy of the backdoored model  $f_{\theta^*}$  on the clean test set  $\mathbf{X}_{\text{test}}$ . For a stealthy backdoor, ABC should remain close to ALC across the SNR range, indicating that the attack does not degrade accuracy on untriggered signals.

To assess the studied threat, we compare the considered adversarial scenario to the attacks Ref1 in [12] and Ref2 in [13]. These attacks were studied in the white-box environment; thus, the assumption about the model and the training process, including the gradient. In addition, these attacks were designed in the digital domain, i.e., after the reception of signals and after the creation of the dataset. A comparison of ALC and ABC for the reference DL models is shown in Fig. 1. As can be observed, the DL models preserve their accuracy on clean signals after being breached (backdoored) across the whole range of SNR values. This is one of the main attributes for backdoor attacks to be stealthy.

To assess all the methods fairly in terms of ASR, the same number of poisoned examples must be considered. Thus, the samples poisoning ratio  $\rho_v$  is considered to be the proportion of the XAI window size (20) to the total number of samples 512, which is approximately  $\rho_v \approx 4\%$ . Therefore, the same poisoning ratio is chosen for both reference attacks. The

TABLE I  
ASR VS. SNR FOR ALL THE STUDIED ATTACKS AGAINST CNN

SNR [dB]	Ref1	Ref2	XAI-guided
-16	22.7%	41.4%	68.7%
-4	39.3%	46.9%	70.6%
8	65.1%	78.2%	79.4%
16	73.6%	80.5%	80.3%

results in Table I show that the XAI-guided attack achieves significantly higher ASR in the low SNR values compared to the reference attacks. These results were obtained against the CNN model. This can be explained by the fact that XAI-guided attack targets the most vulnerable part of the signal, even when the signal is corrupted by noise. In contrast, Ref1 and Ref2 attacks are more easily masked by channel noise, leading to lower ASR at low SNR values. The low SNR values are most critical in modern communication systems, since 5G

and beyond rely on strong channel coding.

To verify the studied attack transferability, the ASR across the reference models is depicted in Fig. 2. The results show

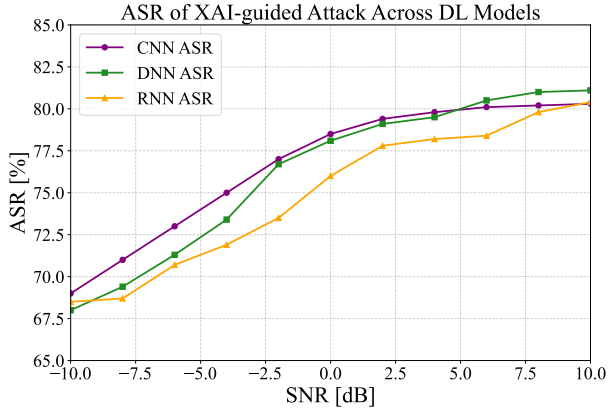


Fig. 2. XAI-guided Attack ASR across DNN, RNN, and CNN

that the studied XAI-guided attack maintains consistently high ASR across all three DL models and over the full SNR range. This indicates that the XAI-guided attack is transferable to other black-box models. At very low SNR values, the CNN already achieves nearly 69% ASR, with the DNN and RNN following closely. As the SNR increases, the ASR rises for all models, reaching approximately 80% at 16 dB for CNN, and slightly higher values for DNN and RNN over 10 dB.

To evaluate the stealthiness of the studied attacks, they are tested against Neural Cleanse [14], STRIP [15], and Activation Clustering [16] defenses, and the results are listed in Table II. The XAI-guided and Ref1 attacks are more stealthy than

TABLE II  
STEALTHINESS RESULTS OF STUDIED ATTACKS AGAINST DEFENSES

Attack	Neural Cleanse	STRIP	Activation Clust
Ref1	1.1	$\Delta\mathcal{H} \approx 0.05, 60\%$	29.3%
Ref2	2.6	$\Delta\mathcal{H} \approx 0.8, 95\%$	72.2%
XAI-guided	[0.92, 1.13]	$\Delta\mathcal{H} \approx 0.02, 54\%$	8.15%

Ref2, where the latter exceeds the anomaly index threshold for Neural Cleanse, which generally equals 2. An entropy gap  $\Delta\mathcal{H}$  of 0.8 with a 95% confidence was observed for the Ref2 attack against STRIP, indicating that STRIP separates clean and triggered distributions. Where for Ref1 and XAI-guided attacks, a lower  $\Delta\mathcal{H}$  was recorded, reflecting partial overlap of entropy distributions. The activation clustering mitigates the Ref2 attack, as was stated in its original paper. The Ref1 attack shows a higher stealthiness against the activation clustering (30% of detection). The XAI-guided attack successfully bypasses the activation clustering defense (8% detection).

#### IV. CONCLUSION

In this work, we studied the vulnerability of DL-based AMC systems to XAI-guided backdoor threats. The triggers were placed in the portions of the signals that are more vulnerable to manipulation using salient regions determined by a customized

low-cost SHAP. Then the trigger value is generated following a combination of class prototypes and principal components. The obtained results show that the studied threat achieves high success rates at low SNR values, making it a solid adversarial attack against modern communication systems. In addition, the studied threat was compared to some of the state-of-the-art threats, and it was found to be more successful and stealthy.

#### REFERENCES

- [1] B. Kim, J. Kim, H. Chae, D. Yoon, and J. W. Choi, "Deep neural network-based automatic modulation classification technique," in *2016 International Conference on Information and Communication Technology Convergence (ICTC)*, 2016, pp. 579–582.
- [2] D. Hong, Z. Zhang, and X. Xu, "Automatic modulation classification using recurrent neural networks," in *2017 3rd IEEE International Conference on Computer and Communications (ICCC)*, 2017, pp. 695–700.
- [3] S.-H. Kim, J.-W. Kim, W.-P. Nwadiugwu, and D.-S. Kim, "Deep learning-based robust automatic modulation classification for cognitive radio networks," *IEEE Access*, vol. 9, pp. 92 386–92 393, 2021.
- [4] D. Adesina, C.-C. Hsieh, Y. E. Sagduyu, and L. Qian, "Adversarial machine learning in wireless communications using rf data: A review," *IEEE Communications Surveys & Tutorials*, vol. 25, no. 1, pp. 77–100, 2022.
- [5] H. Hu, Z. Salcic, L. Sun, G. Dobbie, P. S. Yu, and X. Zhang, "Membership inference attacks on machine learning: A survey," *ACM Computing Surveys (CSUR)*, vol. 54, no. 11s, pp. 1–37, 2022.
- [6] B. Flowers, R. M. Buehrer, and W. C. Headley, "Evaluating adversarial evasion attacks in the context of wireless communications," *IEEE Transactions on Information Forensics and Security*, vol. 15, pp. 1102–1113, 2019.
- [7] S. Kokalj-Filipovic, R. Miller, and J. Morman, "Targeted adversarial examples against rf deep classifiers," in *Proceedings of the ACM Workshop on Wireless Security and Machine Learning*, 2019, pp. 6–11.
- [8] X. Chen, C. Liu, B. Li, K. Lu, and D. Song, "Targeted backdoor attacks on deep learning systems using data poisoning," *arXiv preprint arXiv:1712.05526*, 2017.
- [9] T. Zhao, X. Wang, J. Zhang, and S. Mao, "Explanation-guided backdoor attacks on model-agnostic rf fingerprinting," in *IEEE INFOCOM 2024-IEEE Conference on Computer Communications*. IEEE, 2024, pp. 221–230.
- [10] Y. Salmi and H. Bogucka, "Physical backdoor attack against deep learning-based modulation classification," in *2025 IEEE International Mediterranean Conference on Communications and Networking (Med-ItCom)*, 2025, pp. 1–6.
- [11] T. J. O'Shea, J. Corgan, and T. C. Clancy, "Convolutional radio modulation recognition networks," in *Engineering Applications of Neural Networks: 17th International Conference, EANN 2016, Aberdeen, UK, September 2-5, 2016, Proceedings 17*. Springer, 2016, pp. 213–226.
- [12] Z. Li, H. Jiang, S. Zhang, W. Xiang, and Y. Lin, "Random location poisoning backdoor attack against automatic modulation classification in wireless networks," in *2023 IEEE/CIC International Conference on Communications in China (ICCC)*, 2023, pp. 1–6.
- [13] S. Vavilapalli, N. M. Baishya, B. R. Manoj, and K. Dhaka, "Input agnostic trojan attack for deep learning-based wireless signal classification," in *2024 National Conference on Communications (NCC)*, 2024, pp. 1–6.
- [14] B. Wang, Y. Yao, S. Shan, H. Li, B. Viswanath, H. Zheng, and B. Y. Zhao, "Neural cleanse: Identifying and mitigating backdoor attacks in neural networks," in *2019 IEEE Symposium on Security and Privacy (SP)*, 2019, pp. 707–723.
- [15] Y. Gao, C. Xu, D. Wang, S. Chen, D. C. Ranasinghe, and S. Nepal, "Strip: a defence against trojan attacks on deep neural networks," in *Proceedings of the 35th Annual Computer Security Applications Conference*, ser. ACSAC '19. New York, NY, USA: Association for Computing Machinery, 2019, p. 113–125.
- [16] B. Chen, W. Carvalho, N. Baracaldo, H. Ludwig, B. Edwards, T. Lee, I. Molloy, and B. Srivastava, "Detecting backdoor attacks on deep neural networks by activation clustering," *arXiv preprint arXiv:1811.03728*, 2018.